5.2.2.2 Effect of Gas Velocity

Increasing gas velocity increased the liquid backmixing as well as the liquid dispersion coefficient. The effects of gas velocity in the presence of distributors #1 and #2 at various solids concentrations are shown in a log-log plot of liquid dispersion coefficient gas superficial velocity in Figure 35. All the data at different combinations of distribution plate, solid concentration, and particle size consistently show that the dispersion coefficient increases with increasing gas velocity.

The data shown in Figure 35 can be separated into three different groups. The open circles and hexagons (above the shaped data points) represent the absence of solids. The rest of the open symbols that fall below the shaped data points represent results at high solid concentration. Although the data are scattered, the presence of solid particles clearly decreased the liquid dispersion coefficient. Furthermore the coefficient continues to decrease with increasing solid concentration. Within each solid concentration (0, 5 and 20 lb/ft^3), the results suggest that the type of distributor and the particle size have no effect.

However, without a distributor plate no consistent pattern was observed as a function of gas velocity and solid particle size. Table 14 summarizes the effect of gas velocity and solids on axial dispersion coefficients from the 12-in.-diameter column in the absence of a distributor. In this table, wherever possible, dispersion coefficients were averaged over values obtained at different liquid velocities. When solids were absent, the axial dispersion coefficient increases with gas velocity, as expected. However, the presence of solids complicates the pattern. For both -140 and 20/30 mesh particles, the dispersion coefficient initially increases with gas velocity, but then decreases. Furthermore, at the highest gas velocity employed, the presence of solids decreased in the axial dispersion coefficients. This is in agreement with earlier results obtained in the presence of a distributor. However, at a gas velocity of 0.05 ft/sec, the presence

Figure 35

Liquid Axial Dispersion Coefficient

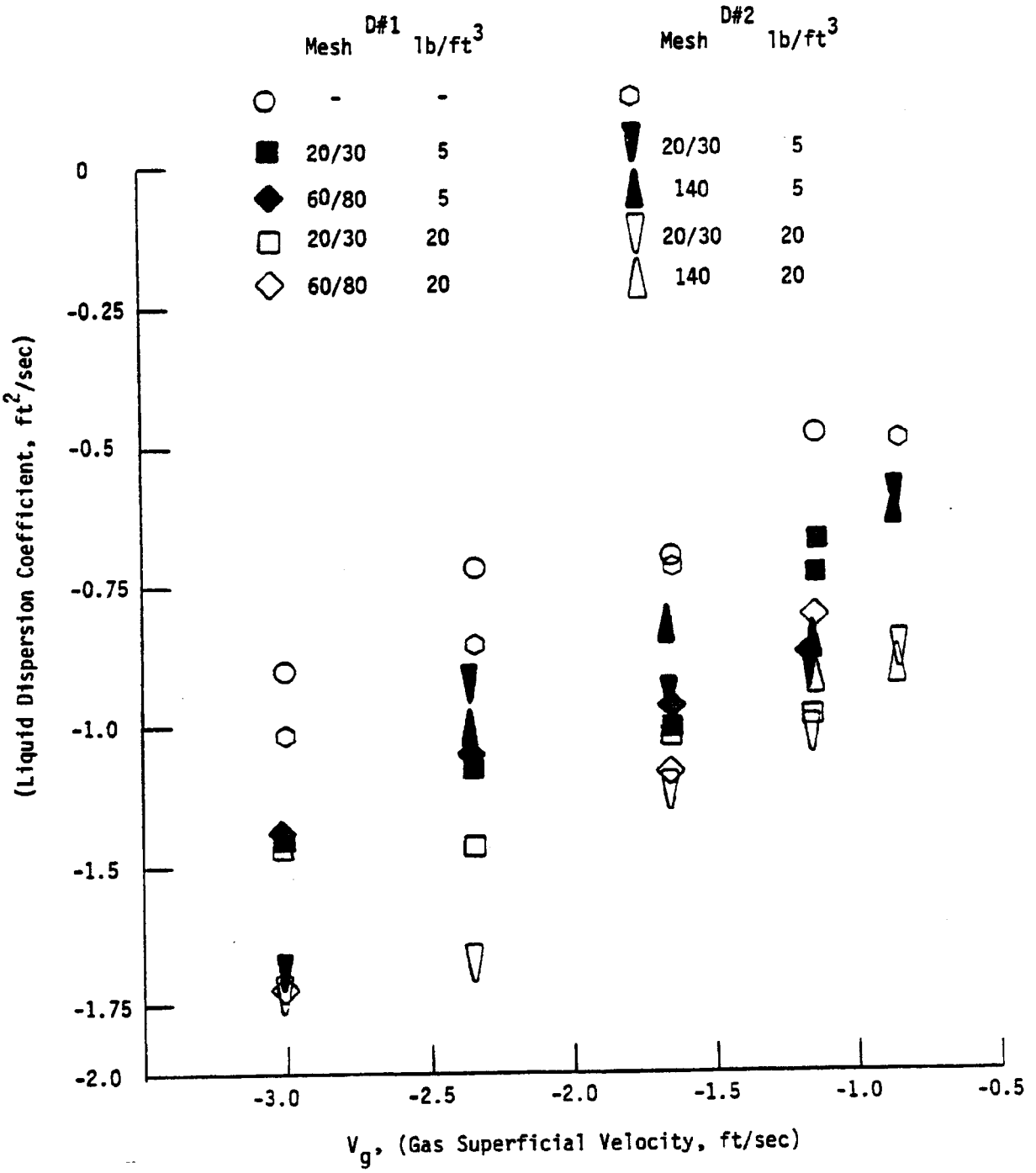

Table 14

Effect of Gas Velocity and Solids on Axial Dispersion Coefficients in the Absence of a Distributor

Gas velocity (ft/sec)	Axial dispersion coefficients (ft^2/sec)		
	No solids	20/30 Mesh Solids	-140 Mesh Solids
0.05	0.277	0.348	0.204
0.10	0.324	--	--
0.194	--	0.458[a]	0.428[a]
0.327	0.494[a]	0.418	0.369

[a] Average values.

of -140-mesh solids decreased the value of the axial dispersion coefficient whereas the presence of 20/30 mesh particles resulted in an increase. These results indicate that the absence of a distributor plate results in some unusual patterns which may be attributed to the surging behavior discussed previously.

5.2.3 Nitrogen/Tetralin and Nitrogen/Tetralin/Sand Systems

Figures 36 to 47 plot the data from data from different dispersion runs in tetralin. Figure 36 shows two runs obtained in the 5-in.-diameter column using the batch method with the tracer injection at the bottom and the top of the column. The square data points were obtained from the samples collected at the top of the column with the dye tracer injected at the column bottom. The circle data points represented the results by reversing the sampling and injection location. As shown in Figure 36, the data obtained from the reversed injection are very close. This run was performed to ensure that the liquid dispersion coefficient (E_{zL}) was not affected by different geometries and inlet conditions. The solid line shows the fit of the axial dispersion model using the least-squares fit technique predicting a value of 0.093 ft^2/sec for E_{zL}.

Figures 37 to 45 show how concentration varies with time for different gas velocities in the 12" column. The data were analyzed by both averaging and least-squares fit techniques described earlier. Comparison of the E_{zL} values obtained from these two methods was summarized in Table 15. The values are very close. Most of the differences between the values are less than 5%. This good comparison provides confidence in the data analyses to determine the E_{zL} values.

Table 15 shows an increase of E_{zL} with increasing gas velocity, though the change is quite insensitive between 0.133 and 0.216 ft/sec gas velocities (illustrated more clearly in Figure 45). In addition, the liquid dispersion coefficient was reduced in the presence of solid particles and with increasing solid concentration. These findings agree with the results from the air/water/sand system.

Figure 36

Comparison of Theoretical and Experimental Concentration

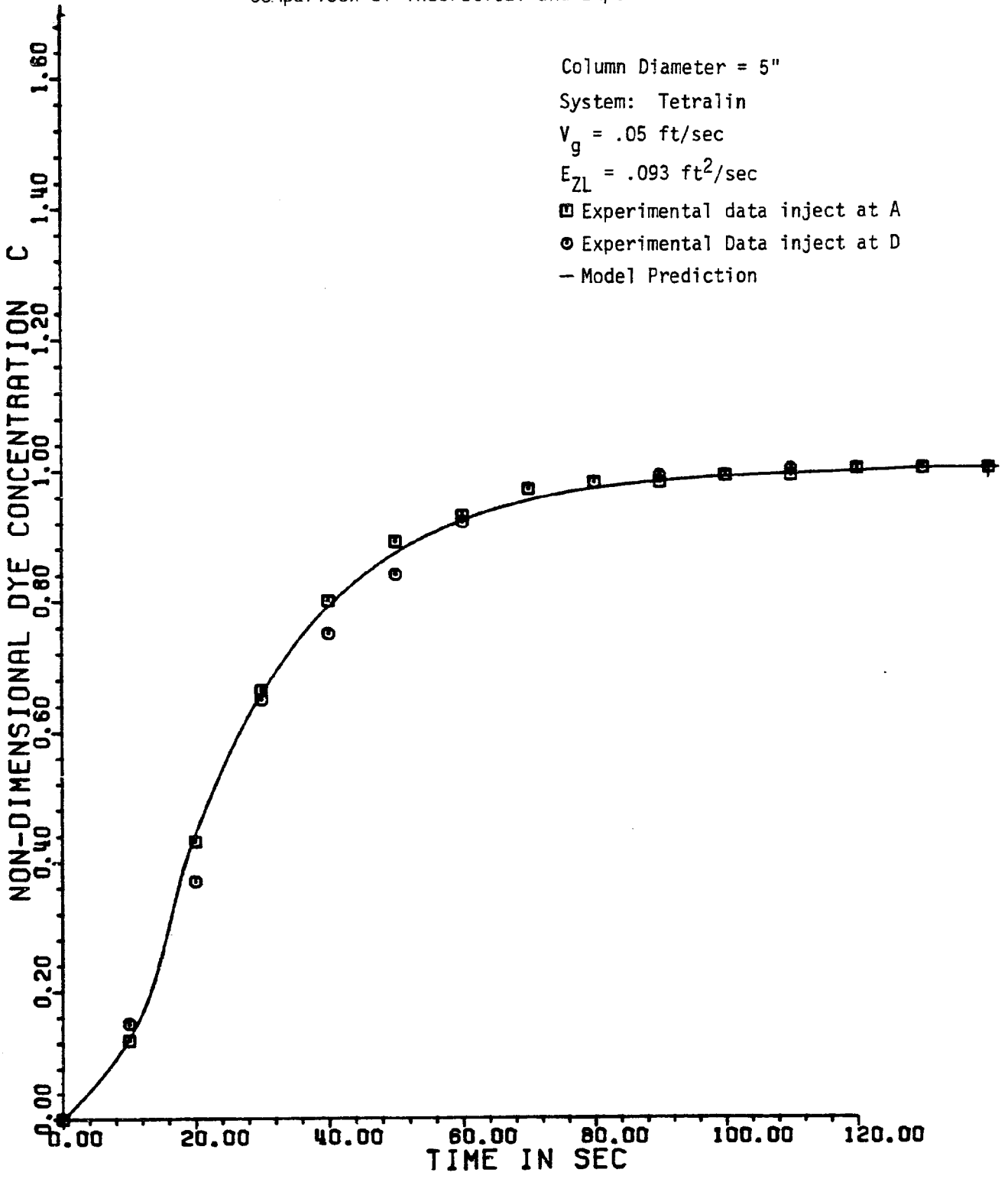

Figure 37

Comparison of Theoretical and Experimental Concentration

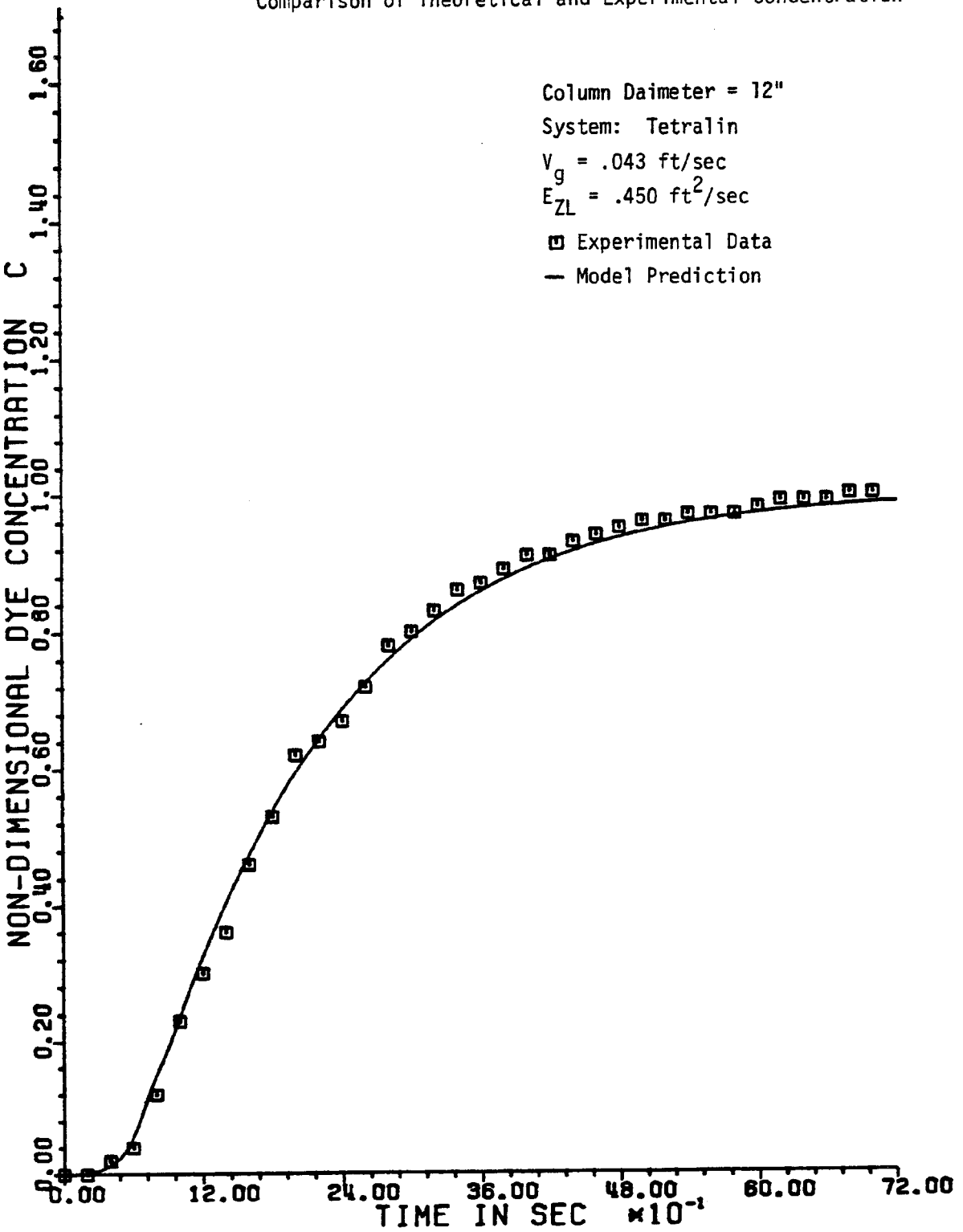

Figure 38

Comparison of Theoretical and Experimental Concentration

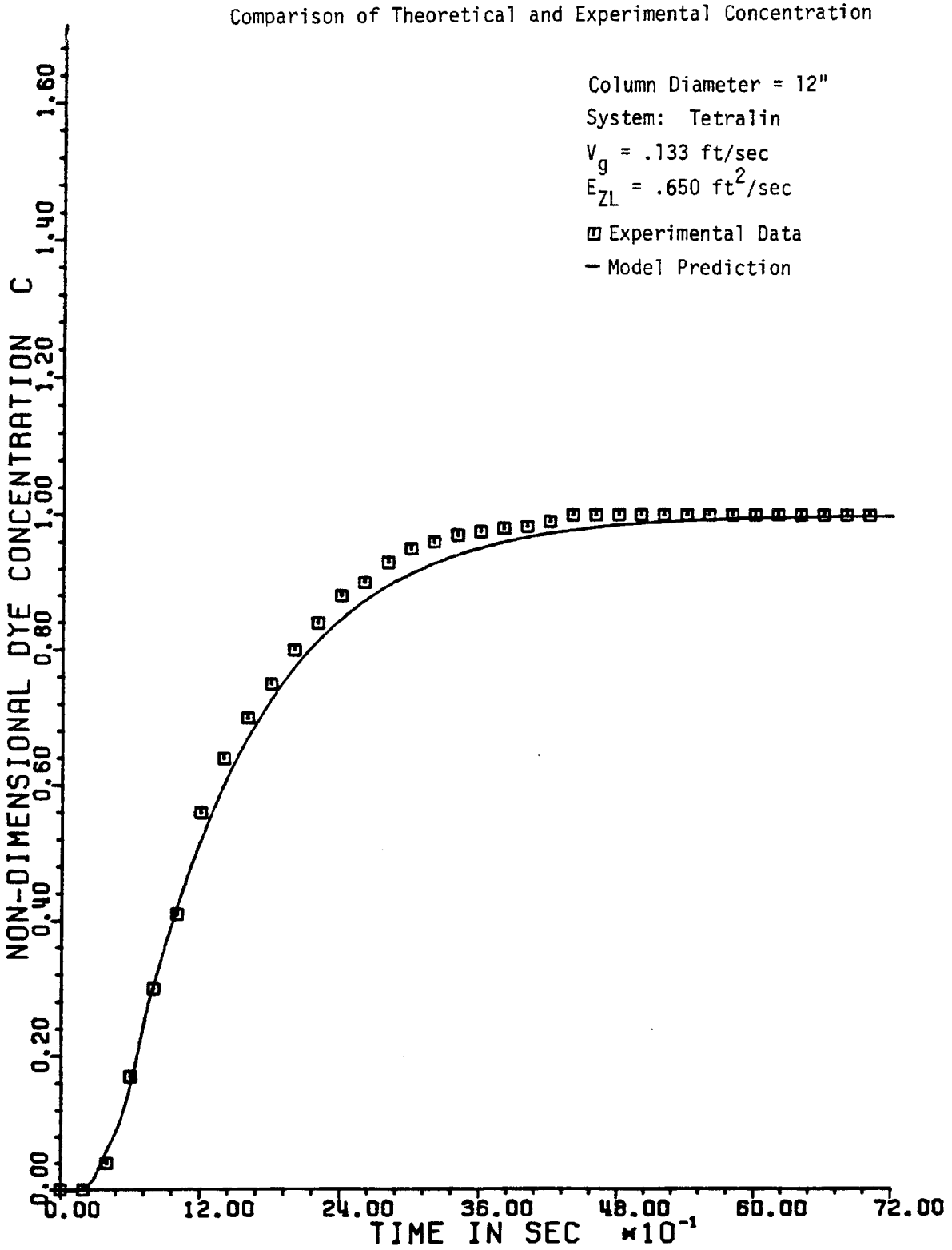

Figure 39

Comparison of Theoretical and Experimental Concentration

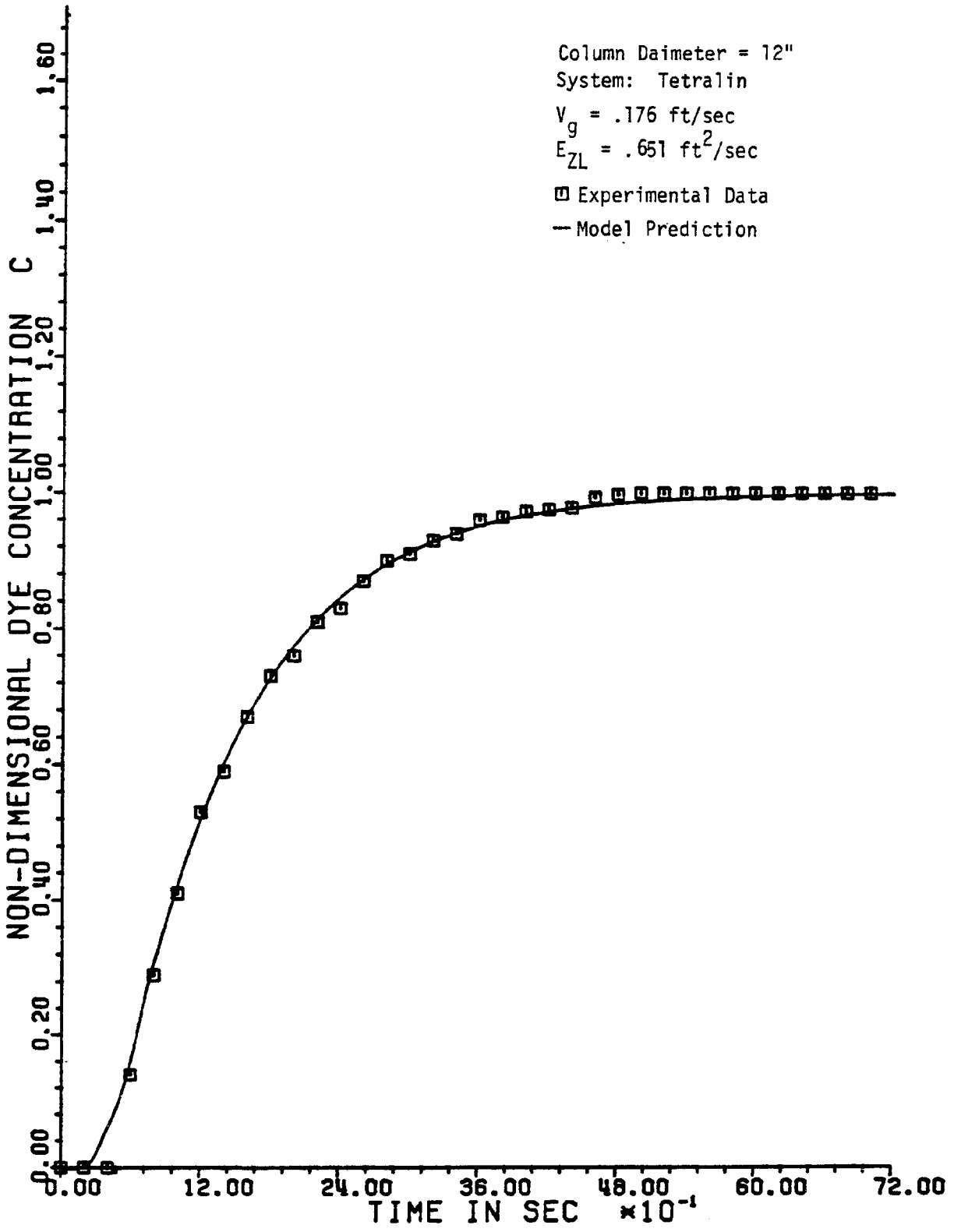

Figure 40

Comparison of Theoretical and Experimental Concentration

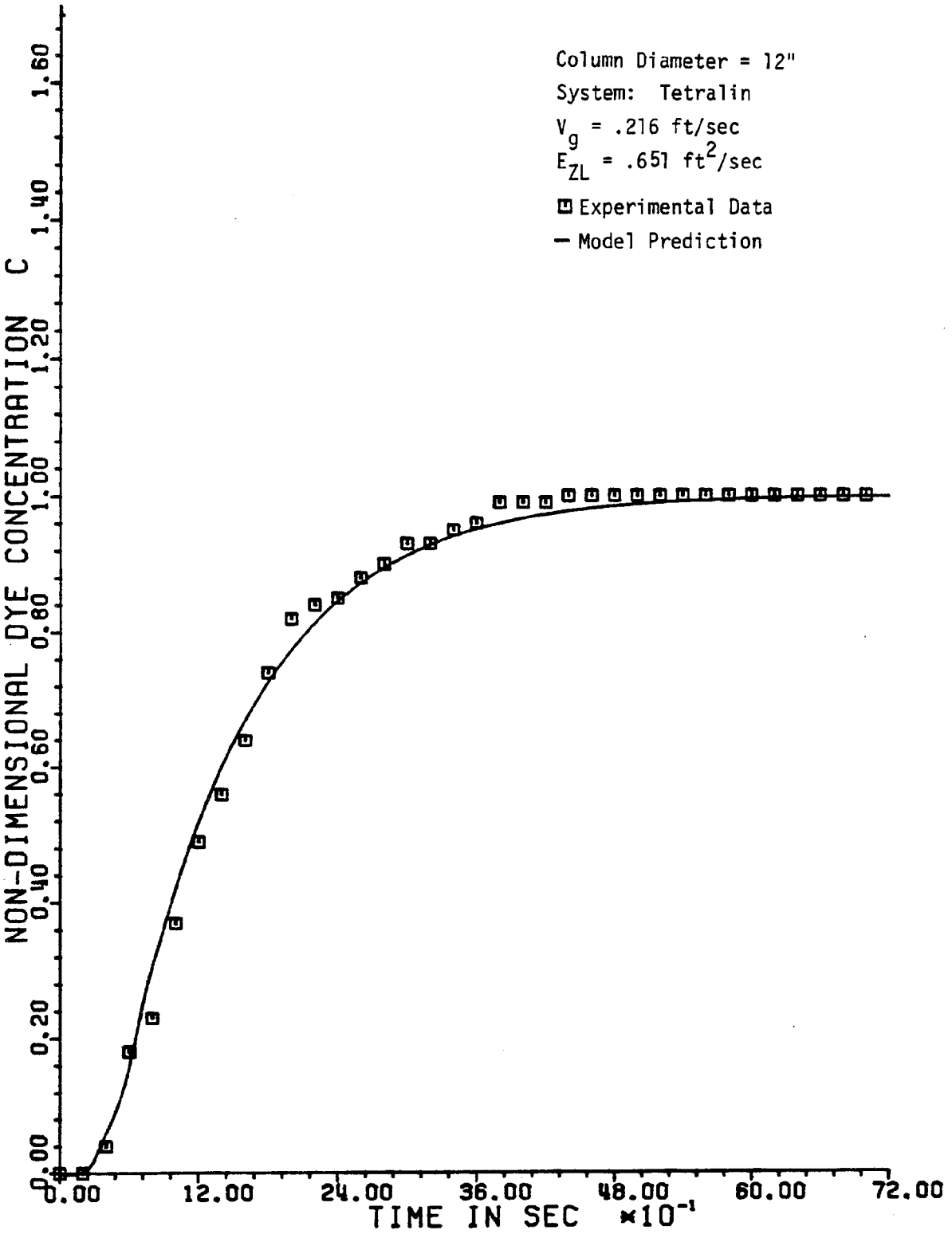

Figure 41

Comparison of Theoretical and Experimental Concentration

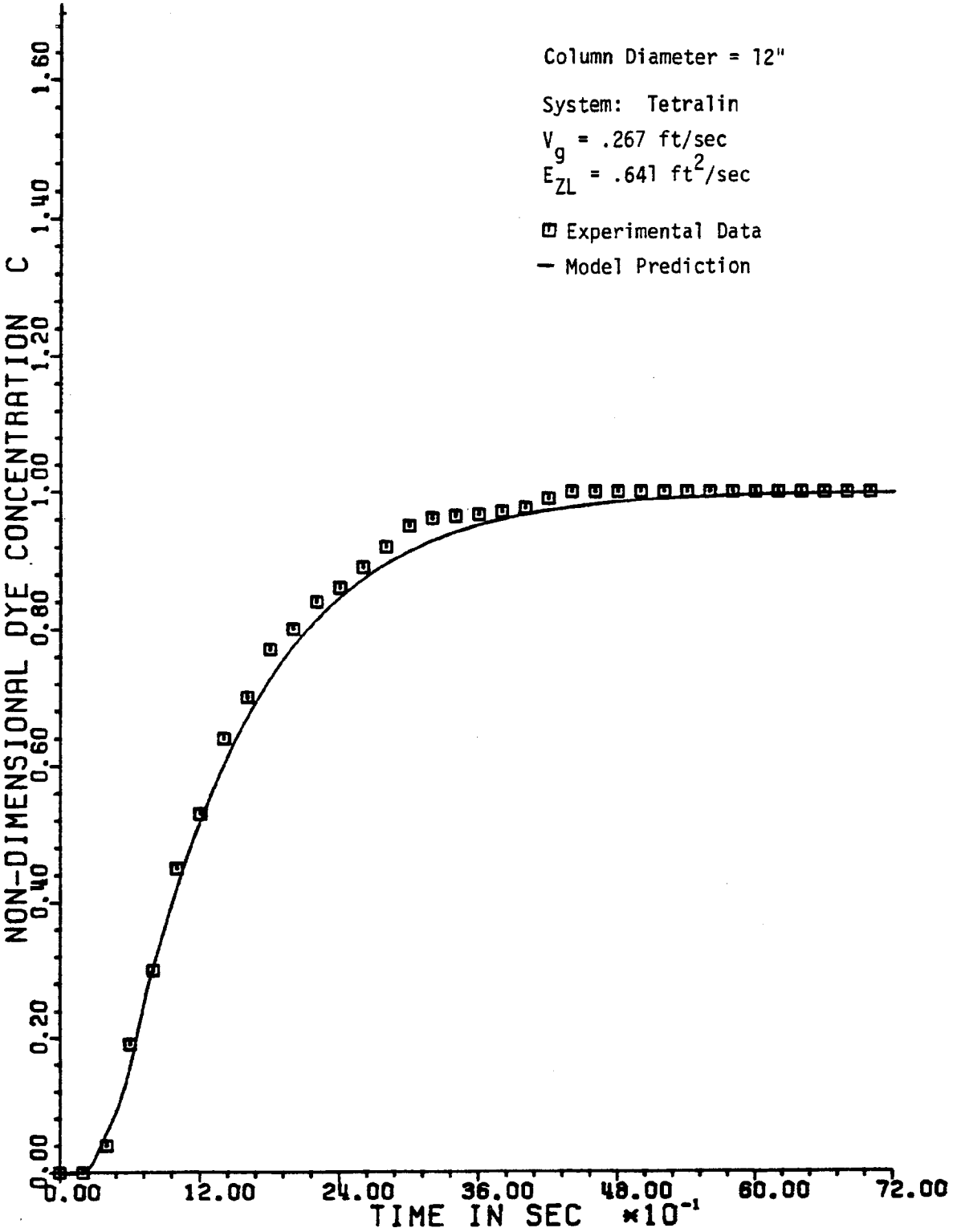

Figure 42

Comparison of Theoretical and Experimental Concentration

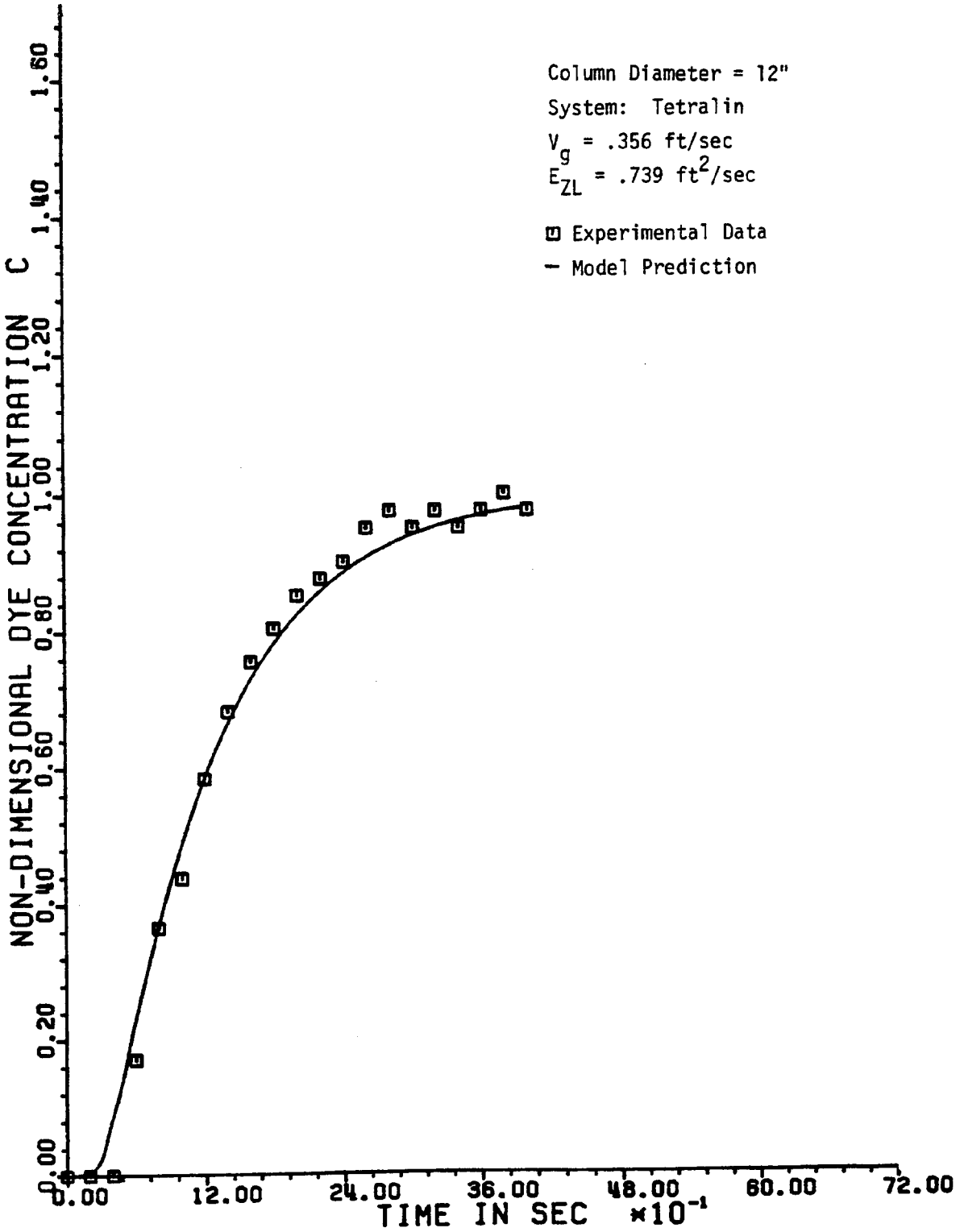

Figure 43

Comparison of Theoretical and Experimental Concentration

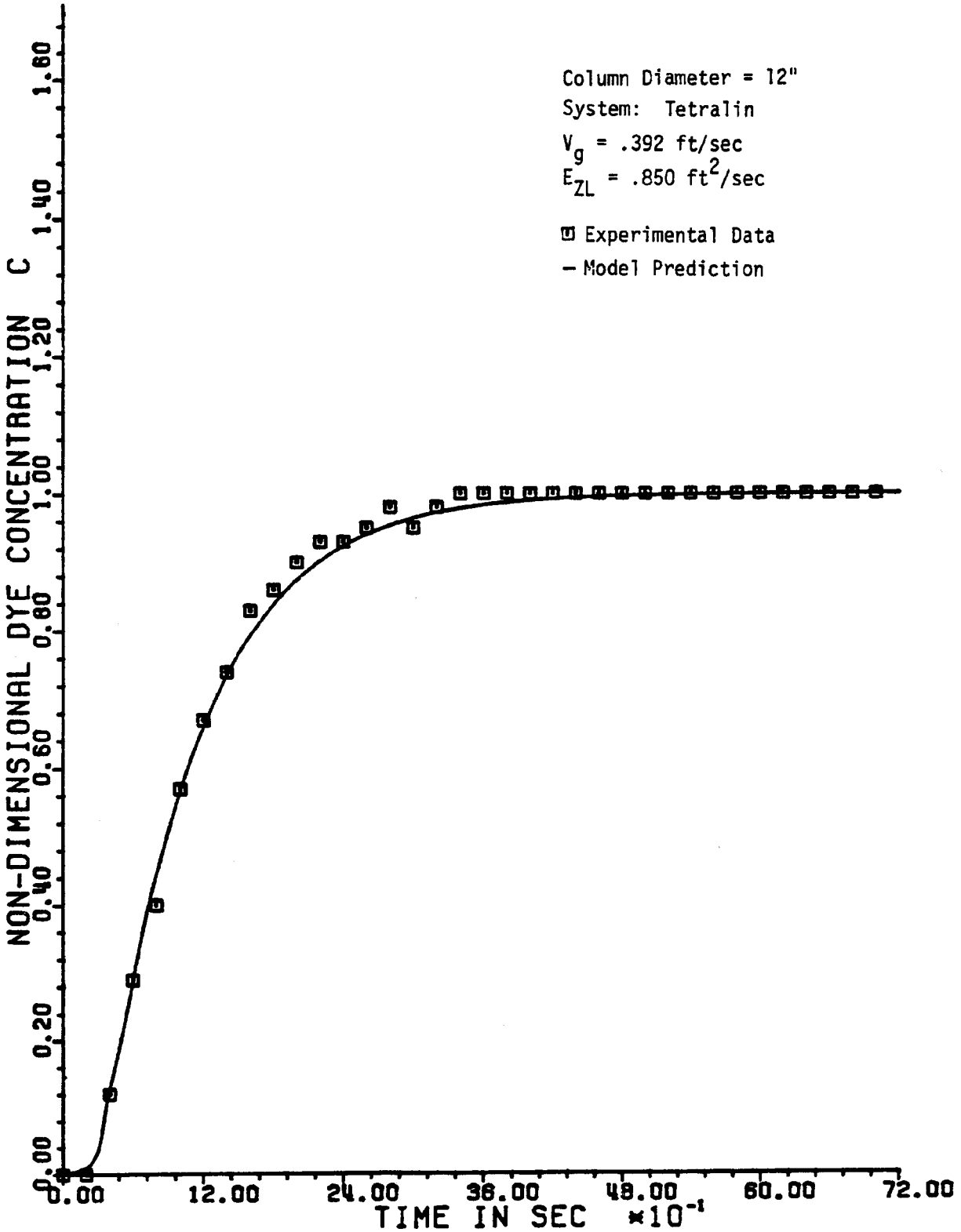

Figure 44

Comparison of Theoretical and Experimental Concentration

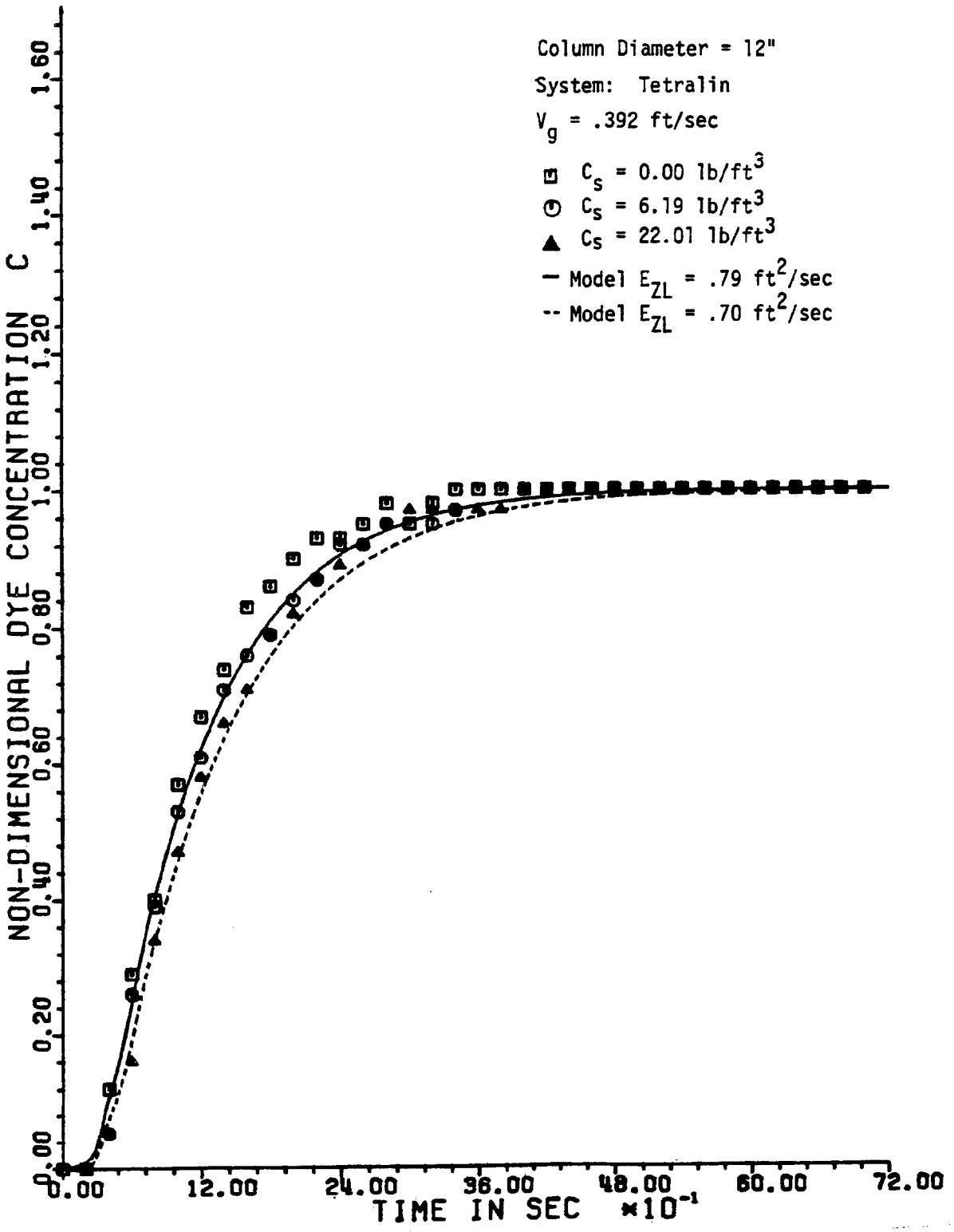

Figure 45

Effect of Gas Velocity on Liquid Dispersion Coefficient

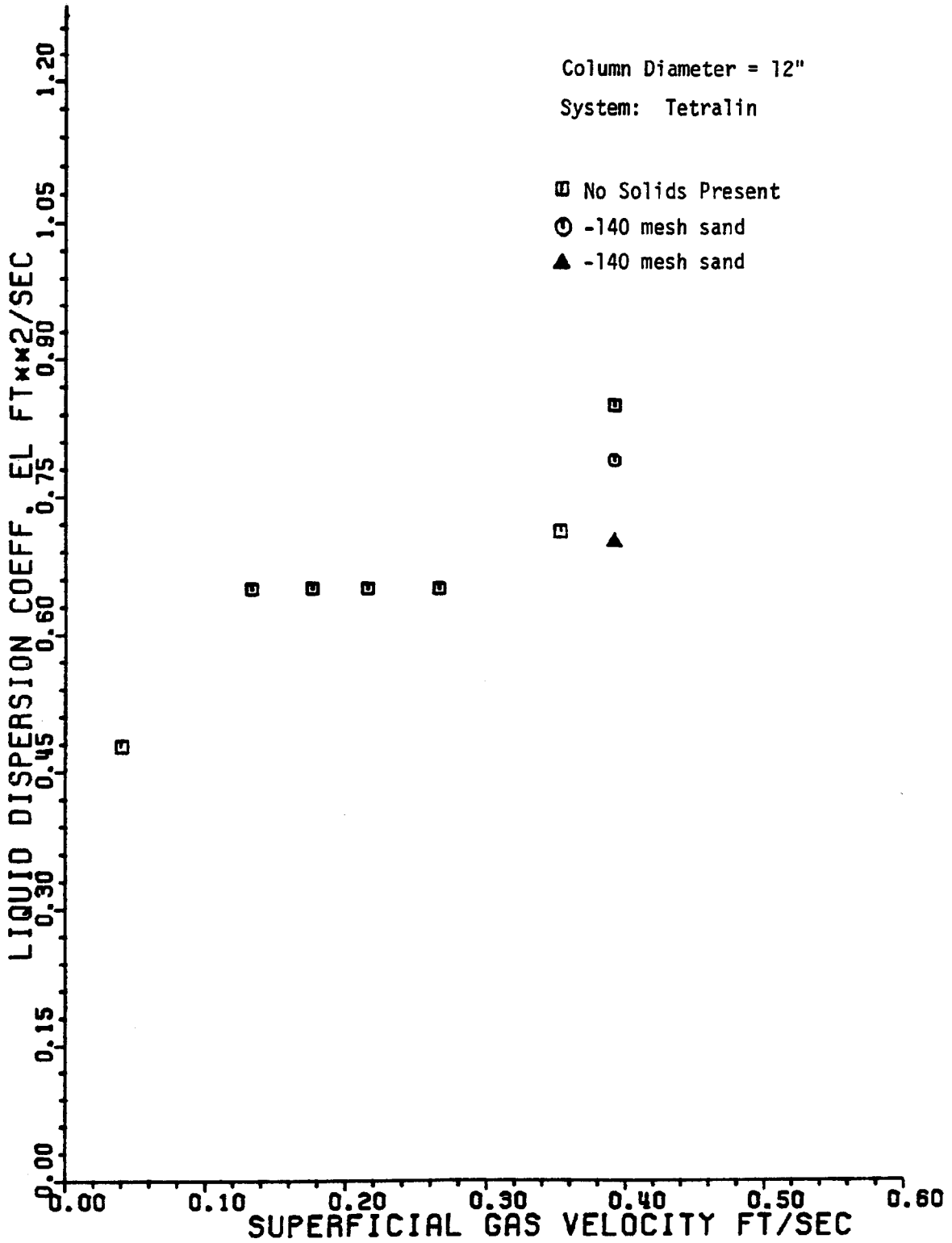

Table 15

Comparison of E_{zL} by Averaging and Least-Squares Fitting Technique

Column diameter (in.)	V_g (ft/sec)	E_{zL} (least sq.)	E_{zL} (averaged)	Remarks
5	0.05	0.0937	0.093	Sampled at D
5	0.05	0.0876	0.093	Sampled at A
12	0.043	0.4503	0.45	
12	0.133	0.6867	0.65	
12	0.176	0.6412	0.651	
12	0.216	0.6393	0.651	
12	0.267	0.6885	0.641	
12	0.356	0.739	--	Averaging was not done
12	0.392	0.8641	0.85	No solids
12	0.392	0.7805	0.79	#140-mesh sand C_2 = 5 lb/ft^3
12	0.392	0.7231	0.70	#140-mesh sand C_s = 22 lb/ft^3

Table 16 summarizes the comparison between the results of these tests and predictions from published correlations. The range of gas velocity simulates those designed for the SRC-I plant, i.e., 0.043-0.392 ft/sec. Each correlation indicates an increase in axial dispersion due to an increase in turbulent mixing resulting from gas agitation of the liquid. These correlations show that diameter, gas velocity, liquid viscosity, and liquid density could influence the values of the axial liquid dispersion coefficient. Of the six correlations compared in Table 16 those of Towel and Baird are the best.

Two additional experiments were run with tetralin using the continuous mode with two liquid velocities (Figures 46 and 47). The following data shows the differences between the continuous and batch modes:

V_g ft/sec	V_l ft/sec	E_{zL} (ft^2/sec) Batch	E_{zL} (ft^2/sec) Continuous
0.392	0.00	0.85	
0.392	0.02		1.02
0.392	0.05		1.33

The E_{zL} values for the continous operation mode were determined by matching the peak time between the tracer curve and the model as described in the experimental section. Unlike the sodium chloride tracer test in the air/water system, the dye tracer study requires discrete samples collected at fixed interval of time. Usually, a flat region exists at the top of the graph which makes the resolution of which point is an assumed peak rather questionable. In fact the curve fits shown in Figures 46 and 47 were poor. Since limited runs in continuous operation mode can be performed with tetralin due to accumulation of dye concentration, effect of liquid flow was not studied at other gas velocity. At this point in time, little can be said about liquid velocity effect on E_{zL} in tetralin system. Since the air/water system had determined that there is practically no liquid flow effect on E_{zL}, it is unlikely that the physics will change in the tetralin system.

Table 16

Comparison of Experiments and Correlations
for Tetralin Liquid Dispersion Coefficient

Column Diameter (in.)	V_g (ft/sec)	E_{zL} Exp.	E_{zL} (Towel)	E_{zL} (Cova)	E_{zL} (Deckwer)	E_{zL} (Hikita)	E_{zL} (Baird)	E_{zL} (Ying)
5	0.05	0.093	0.074	0.176	0.081	0.155	0.128	0.088
12	0.043	0.45	0.255	0.167	0.268	0.447	0.390	0.264
12	0.133	0.65	0.449	0.240	0.370	0.627	0.565	0.397
12	0.176	0.65	0.516	0.263	0.403	0.701	0.620	0.439
12	0.216	0.65	0.572	0.281	0.428	0.767	0.664	0.472
12	0.276	0.65	0.636	0.300	0.456	0.846	0.712	0.516
12	0.392	0.85	0.770	0.340	0.512	1.028	0.808	0.585

Figure 46

Dimensionless Concentration Versus Dimensionless Time

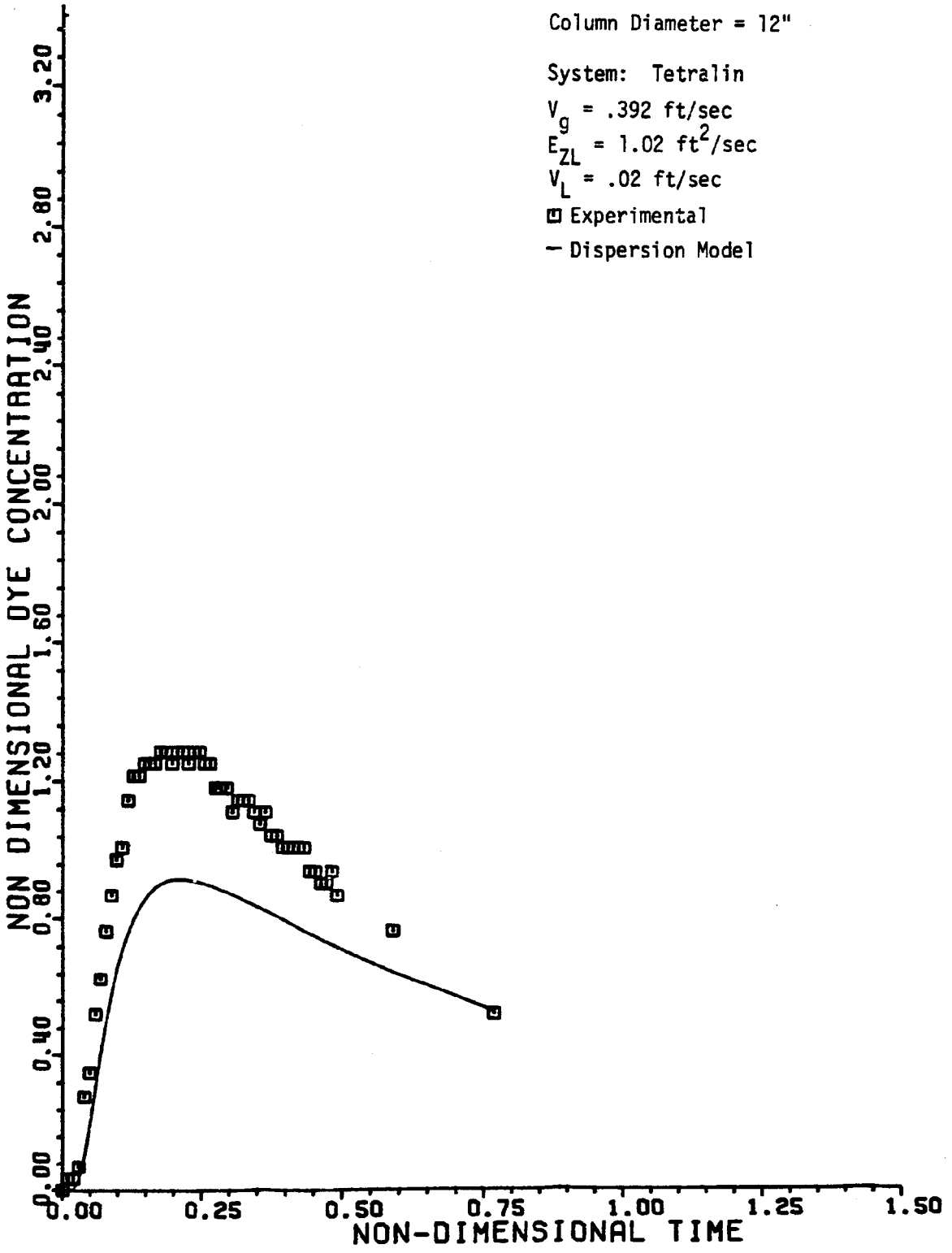

Figure 47

Dimensionless Concentration Versus Dimensionless Time